Electronic Supplementary Information: Optical and Dielectric Properties of Lead Perovskite and Iodoplumbate Complexes: An *Ab initio* Study

Malladi Srikanth,* Mailde S. Ozório,* and Juarez L. F. Da Silva*

São Carlos Institute of Chemistry, University of São Paulo, PO Box 780, 13560 – 970, *São Carlos, SP, Brazil*

E-mail: smalladi@iqsc.usp.br; mailde.s.ozorio@usp.br; juarez_dasilva@iqsc.usp.br

1 Introduction

The present electronic supporting information (ESI) contains complementary data, analyses, figures, and tables, namely, (*i*) additional computational technical details; (*ii*) definition for the geometrical and lattice parameters analyses for the pseudo-cubic; (*iii*) convergence tests as a function of the cutoff energy and number of **k**-points; (*iv*) orthorhombic (1D, 3D), and hexagonal $A\mathrm{PbI_3}$ structures; (*iv*) finally, additional data for the optical and electronic properties.

2 Structural, Energetic, and Electronic Analyses

2.1 Goldschmidt's Tolerance Factor

The formability of perovskites, ABX_3, can be empirically estimated through the Goldschmidt's tolerance factor, TF,[1] which is given by the following equation,

$$TF = \frac{r_A + r_X}{\sqrt{2}(r_B + r_X)} \ , \tag{1}$$

where r_A, r_B and r_X are the ionic radii for the ions in the A, B and X sites, respectively. In general an ideal cubic perovskite structure TF ranges from 0.9 to 1.0, while for distorted quasi-cubic perovskite structures the TF range from 0.8 to 0.9, and for the hexagonal phase, $TF > 1$. From Table 1, the ammonium (AM) and dabconium (DA) cations, the TF values are not in the range of perovskite formation region, while for the Cs-, MA- and FA-cations have a favorable TF for the formation of perovskite structures.

Table 1: Lead iodide $\boldsymbol{A}\mathbf{PbI_3}$ perovskites with different $\boldsymbol{A}$-cations, radius, tolerance-factor, TF,[2] at room-temperature (RT) phase. We considered the following cations, $\boldsymbol{A} = \mathbf{Cs^+}$, ammonium (AM), $\mathbf{[NH_4]^+}$, methylammonium (MA), $\mathbf{[CH_3NH_3]^+}$, formamidinium (FA), $\mathbf{[NH_2(CH)NH_2]^+}$, and dabconium (DA), $\mathbf{[C_6H_{13}N_2]^+}$.

Property	Cs	AM	MA	FA	DA
Radius (Å)	1.67	1.46	2.17	2.53	3.39
TF	0.80	0.76	0.91	1.02	1.17
RT phase	Orthorhombic	Orthorhombic	Tetragonal	Cubic and Hexagonal	Hexagonal
Color	yellow	yellow	black	balck and yellow	yellow

2.2 Effective Coordination Concept

In this work, we employed the effective coordination concept,[3,4] which is useaful approach to perform the analysis of the coordination number and average weighted bond lengths. The

perfect PbI_6 has have 6-coordination in $MAPbI_3$ at Pb−I bond length approximately 3.17 Å, and ECN decreases as with inclusion lighter element chlorine.[5] The PbI_6 pseudo-octahedron bond angles and ECN effected by the MA cation rotation. The equations employed for the ECN is given below,

$$ECN^{\mathrm{Pb}} = \sum_j Exp\Big[1 - \Big(\frac{d_{ij}}{d^i_{av}}\Big)^6\Big] \ , \tag{2}$$

where

$$d^i_{av} = \frac{\sum\limits_j d_{ij} Exp\Big[1 - \Big(\frac{d_{ij}}{d_i^{min}}\Big)^6\Big]}{\sum\limits_j Exp\Big[1 - \Big(\frac{d_{ij}}{d_i^{min}}\Big)^6\Big]} \ . \tag{3}$$

d_{ij} indicates the distance between the atoms i and j, while d_i^{min} indicates the minimum distance between i and the nearest neighbour atom.

2.3 Bond Angle Variance

The bond angle variance,[6] was calculated using the following equation,

$$BAV = \frac{1}{a-1}\sum_{i=1}^{a}\left(\phi_i - \phi_0\right)^2, BAV = \sum_{i=1}^{12}\frac{\left(\phi_i - 90^0\right)^2}{11} \ , \tag{4}$$

where ϕ_i is the i^{th} bond angle, and ϕ_0 is the ideal bond angle for a regular octahedron.

2.4 Cohesive and Formation Energies

The cohesive energy is the difference between the total energy of a solid to its constituent free atoms and this represents chemical stability of the solid. The cohesive energy of organic-inorganic perovskite defined as the energy required to separate organic molecule and inorganic species to infinite distance from each other. We employed the following equation,

$$E_{coh} = E^{\mathrm{MAPbI_3}}_{tot} - iE^{\mathrm{C}}_{tot} - jE^{\mathrm{N}}_{tot} - kE^{\mathrm{H}}_{tot} - mE^{\mathrm{I}}_{tot} - nE_{\mathrm{Pb}} \ , \tag{5}$$

where $E_{tot}^{\mathrm{MAPbI_3}}$ is the total energy of the $MAPbI_3$ perovskite, while the ramining terms indicate the total energy of the respective free atoms. All the calculations are performed using the same cutoff energy.

Furthermore, we calculated also the formation energy, which is defined as follows. Formation energy of a substance is the change of energy between the final products to its initial reactants. Our DFT calculations are 0 K temperature calculations, and hence, entropy term not included in the calculation of formation enthalpy. The following chemical reactions can be represented,

$$\mathrm{MAI_{(solid)}} + \mathrm{PbI_{2(solid)}} \longrightarrow \mathrm{MAPbI_{3(solid)}} \ , \tag{6}$$

$$\mathrm{MAI_{(gas)}} + \mathrm{PbI_{2(solid)}} \longrightarrow \mathrm{MAPbI_{3(solid)}} \ . \tag{7}$$

Thus, the formation can be calculated using the following equation,

$$\Delta H_f(A\mathrm{PbI_3}) = E_{tot}^{A\mathrm{PbI_3}} - E_{tot}^{A\mathrm{I}} - E_{tot}^{\mathrm{PbI_2}} \ . \tag{8}$$

2.5 Optical Properties

The optical band gap and optical dielectric constant was calculated in the long-wavelength limit ($q \to 0$) by sufficiently increasing the empty states (`NBANDS` = 2×`NELECT`) within the independent particle approach by excluding the local field effects as prescribed in Gajdoš *et al*[7] work. The convergence of dielectric function for $CsPbI_3$ was observed at 80 $\mathrm{\AA}^{-1}$, Figure 6, dense **k**-mesh/grid is necessary to integrate the Brillouin zone to attain accurate linear response properties.[8] The optical properties and interband transitions of the perovskites calculated from the dielectric responses of ε_2 and ε_1 derived by summation over empty states and Kramer–Krönig[7,9] relation using small complex shift of 0.01 eV for various polymorphs of $APbI_3$. The band to band transition amplitudes calculated by using our in-house code.[10]

$$\varepsilon^{(2)}_{\alpha\beta}(\omega) = \frac{4\pi^2 e^2}{\Omega} lim_{q\to 0} \frac{1}{q^2} \sum_{c,v,\mathrm{k}} 2\omega_{\mathrm{k}} \delta(\varepsilon_{c\mathrm{k}} - \varepsilon_{v\mathrm{k}} - \omega) \times \langle u_{c\mathrm{k}+e_\alpha q} | u_{v\mathrm{k}} \rangle \langle u_{c\mathrm{k}+e_\beta q} | u_{v\mathrm{k}} \rangle \qquad (9)$$

where, c and ν represents the conduction and valence band states, u_{ck} is cell periodic part of the orbitals at the k-point, e is the electronic charge, Ω is the volume and ω is the light frequency.

3 Computational Convergence Tests

To obtain accurate results in the present study, we performed several computational convergence tests, which includes the following calculations: equilibrium lattice parameters (a_0, b_0, c_0) as a function of the number of **k**-points in the irreducible part of the Brillouin zone (represented by the **k**-density or **k**-mesh) and number of plane-waves employed to the expansion of the Kohn–Sham orbitals (i.e., cutoff energy - `ENCUT`). The results are summarized below in Tables 2 and 3.

Table 2: The calculated lattice parameters (a_0, b_0, c_0), cubic deviation, and relative stabilization energy of MA [100] oriented pseudo-cubic $CH_3NH_3PbI_3$ as a function of the number of k-points (k-density) using the PBE functional and a cutoff energy of 842 eV**.**

k-density (Å^{-1})	**k**-mesh $n\times n\times n$	a_0 (Å)	b_0 (Å)	c_0 (Å)	CD (Å)	ΔE_{tot} meV
20	3×3×3	6.44	6.50	6.40	0.10	100.08
30	5×5×5	6.43	6.52	6.49	0.14	5.75
40	6×6×6	6.42	6.52	6.54	0.21	−1.35
50	8×8×8	6.43	6.52	6.51	0.17	−0.09
60	9×9×9	6.42	6.52	6.54	0.21	0.30
70	11×11×11	6.42	6.52	6.54	0.22	0.16
80	12×12×12	6.42	6.52	6.54	0.23	0.00

Table 3: The MA [100] oriented pseudo-cubic structure local geometrical parameters such as Pb−I bond length, cis I−Pb_{av}-I bond angle and SD, bond angle variance (BAV), ECN, PbI_6 octahedral volume, and average H-bond lengths calculated by using PBE functional at different k-density

k-density ($Å^{-1}$)	$Pb-I_{av}$ (Å)	$I-Pb_{av}$-I (°)	BAV ($°^2$)	ECN^{Pb} (NNN)	Vol^{Pb} ($Å^3$)	$N_{H...I}$ (Å)	$C_{H...I}$ (Å)
20	3.22	90.30 ± 2.51	6.33	5.97	44.60	2.70 ± 0.09	3.51 ± 0.05
30	3.25	89.90 ± 5.00	25.03	5.74	45.37	2.69 ± 0.07	3.55 ± 0.10
40	3.26	89.83 ± 6.07	36.90	5.57	45.61	2.69 ± 0.06	3.57 ± 0.13
50	3.26	89.86 ± 5.61	31.47	5.64	45.51	2.69 ± 0.06	3.56 ± 0.12
60	3.26	89.84 ± 6.04	36.56	5.58	45.59	2.69 ± 0.06	3.57 ± 0.13
70	3.26	89.83 ± 6.05	36.66	5.57	45.59	2.69 ± 0.06	3.57 ± 0.13
80	3.26	89.83 ± 6.06	36.71	5.57	45.54	2.69 ± 0.06	3.57 ± 0.13

Table 4: The MA [100] oriented $CH_3NH_3PbI_3$ pseudo-cubic lattice parameters, cubic deviation, and relative stabilization energy calculated using a cutoff energy of $1052\,\mathrm{eV}$, using the PBE functional, and with a k-density of $40\,Å^{-1}$ for the Brillouin zone integration.

Cutoff energy (eV)	a_0 (Å)	b_0 (Å)	c_0 (Å)	CD (Å)	ΔE_{tot} (meV)
421	6.28	6.39	6.33	0.16	195.11
526	6.40	6.48	6.47	0.15	34.30
631	6.41	6.51	6.50	0.19	9.59
736	6.42	6.51	6.53	0.19	2.55
842	6.42	6.52	6.54	0.21	0.53
947	6.43	6.52	6.53	0.20	−0.31
1052	6.43	6.51	6.55	0.20	0.00

Table 5: The MA [100] oriented $CH_3NH_3PbI_3$ pseudo-cubic local geometrical parameters, Pb−I bond length, cis I−Pb−I average bond angle and SD, BAV, ECN, PbI_6 octahedral volume, and average H-bond lengths calculated by using PBE functional and k-density of $40\,\text{Å}^{-1}$.

Cutoff Energy (eV)	$Pb-I_{av}$ (Å)	$I-Pb_{av}-I$ (°)	BAV ($°^2$)	ECN^{Pb} (NNN)	Vol^{Pb} ($Å^3$)	$N_{H...I}$ (Å)	$C_{H...I}$ (Å)
421	3.18	89.97 ± 6.25	39.01	5.92	42.26	2.69 ± 0.02	3.42 ± 0.07
526	3.24	89.87 ± 5.67	32.20	5.74	44.71	2.69 ± 0.06	3.53 ± 0.08
631	3.25	89.86 ± 5.99	35.91	5.69	45.15	2.70 ± 0.05	3.57 ± 0.10
736	3.26	89.84 ± 5.90	34.79	5.60	45.48	2.69 ± 0.06	3.55 ± 0.12
842	3.26	89.83 ± 6.07	36.90	5.57	45.61	2.69 ± 0.06	3.57 ± 0.13
947	3.26	89.84 ± 6.15	37.91	5.58	45.63	2.69 ± 0.05	3.58 ± 0.13
1052	3.26	89.83 ± 6.00	35.99	5.55	45.68	2.69 ± 0.06	3.56 ± 0.13

4 Cubic Structures with Different Orientations for the *A*-cations: Cs, AM, MA, FA, DA

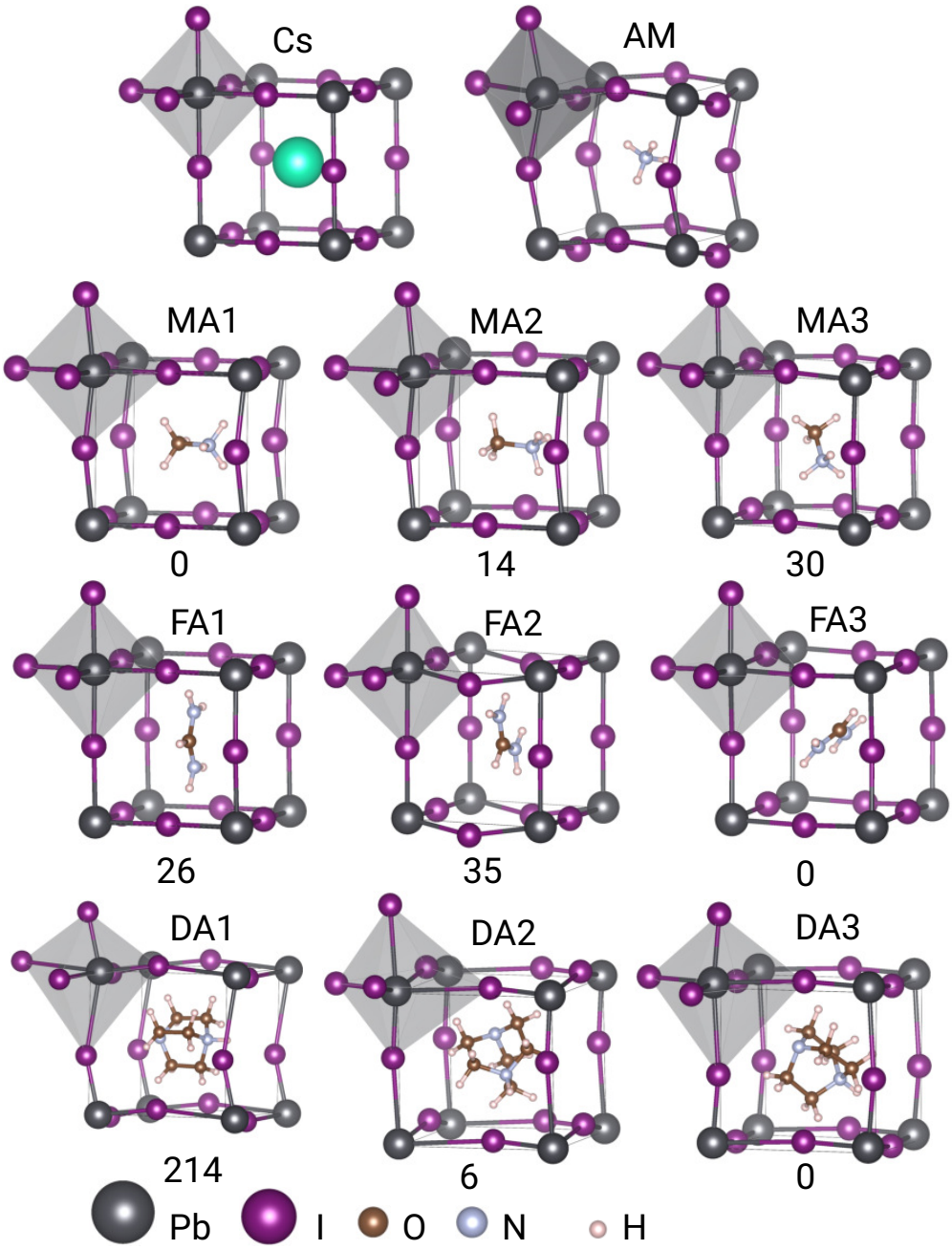

Figure 1: The cubic perovskite having the central cation of (a) Cs; the pseudo-cubic cage of PbI_3 with organic cations with distinct molecular orientations (b) ammonium (AM), (c-e) methylammonium (MA), (f-h) formamidinium (FA), and (i-k) dabconium (DA), respectively, relative stabilization energies are given in meV

5 Structural Parameters, Total Energy, and Energy Bandgap, for Different *A*-cation Orientations (APbI$_3$): MA, FA, DA

Below, we summarize the structural parameters, total energy, and energy band gap for all A-cations and different crystal structures.

5.1 MAPbI$_3$: Pseudo-cubic Structure

Table 6: MAPbI$_3$ perovskite pseudo-cubic crystal lattice parameters, cell volume, density, effective coordination number(ECN), quadratic elongation (QE), bond angle variance (BAV), total energy per formula unit, E_{tot}, relative stabilization energy (R.E) and energy bandgap calculated at PBE+D3 and $40\,\text{Å}^{-1}$.

Property	MA1	MA2	MA3
a_0 (Å)	6.30	6.37	6.40
b_0 (Å)	6.40	6.35	6.33
c_0 (Å)	6.36	6.39	6.33
V (Å^3/f.u)	256.48	257.92	255.99
Density (g cm^{-3})	4.01	3.99	4.02
PbI$_6$ vol. (Å^3)	42.75	42.99	42.66
AI$_{12}$ vol. (Å^3)	217.32	217.22	216.49
Ratio (AI$_{12/}$PbI$_6$)	5.08	5.05	5.07
ECN^{Pb}	5.89	5.86	5.96
ECN^{A}	9.63	9.56	10.53
Avg. Pb–I (Å)	3.19	3.19	3.18
Avg. Pb–I–Pb (°)	168.73	170.89	172.40
QE	1.0104	1.0079	1.0048
BAV (°^{2})	35.49	26.31	16.32
E_{tot} (eV)	−51.89	−51.87	−51.86
R.E (meV) per f.u	0	14	30
E_g (eV) at G (0,0,0)	4.50	4.51	4.52

5.2 $FAPbI_3$: Pseudo-cubic Structure

Table 7: $FAPbI_3$ perovskite pseudo-cubic crystal lattice parameters, cell volume, density, effective coordination number (ECN), quadratic elongation (QE), bond angle variance (BAV), total energy per formula unit (E_{tot}), relative stabilization energy (R.E) and bandgap (E_g) calculated at PBE+D3 and $40\,\text{Å}^{-1}$.

Property	FA1	FA2	FA3
a_0 (Å)	6.49	6.53	6.31
b_0 (Å)	6.32	6.54	6.61
c_0 (Å)	6.38	6.29	6.32
V (Å^3/f.u)	261.81	268.68	263.91
Density (g cm^{-3})	4.01	3.91	3.98
PbI_6 vol. (Å^3)	43.63	44.78	43.63
AI_{12} vol. (Å^3)	220.61	230.17	223.84
Ratio ($AI_{12/}PbI_6$)	5.06	5.14	5.09
ECN^{Pb}	5.97	5.36	5.57
ECN^{A}	10.89	9.49	11.49
Avg. Pb–I (Å)	3.20	3.25	3.22
Avg. Pb–I–Pb (°)	175.80	170.81	169.20
QE	1.0026	1.0189	1.0119
BAV (°^{2})	8.29	56.73	33.18
E_{tot} (eV)	−56.59	−56.58	−56.61
R.E (meV) per f.u	26	35	0
E_g (eV) at G (0,0,0)	3.72	3.72	3.80

5.3 $DAPbI_3$: Pseudo-cubic Structure

Table 8: $DAPbI_3$ perovskite pseudo-cubic crystal lattice parameters, cell volume, density, effective coordination number (ECN), quadratic elongation (QE), bond angle variance (BAV), total energy per formula unit (E_{tot}), relative stabilization energy (R.E) and bandgap (E_g) calculated at PBE+D3 and $40\,\text{Å}^{-1}$.

Property	DA1	DA2	DA3
a_0 (Å)	7.11	6.87	7.00
b_0 (Å)	6.81	6.77	7.03
c_0 (Å)	7.30	7.29	7.03
V (Å^3/f.u)	353.03	338.64	346.10
Density ($\text{g}\,\text{cm}^{-3}$)	3.30	3.44	3.36
PbI_6 vol. (Å^3)	58.84	56.44	57.68
AI_{12} vol. (Å^3)	303.93	292.58	298.55
Ratio ($AI_{12/}PbI_6$)	5.17	5.18	5.18
ECN^{Pb}	3.06	3.23	3.09
ECN^{A}	10.32	8.88	10.37
Avg. Pb–I (Å)	3.59	3.52	3.52
Avg. Pb–I–Pb (°)	160.69	165.35	169.82
QE	1.0570	1.0407	1.0284
BAV (°^{2})	103.60	3.23	28.39
E_{tot} (eV)	−130.45	−130.66	−130.67
R.E (meV) per f.u	214	6	0
E_g (eV) at G (0,0,0)	3.95	3.76	4.41

5.4 $MAPbI_3$: Orthorhombic-3D Structure

Table 9: $MAPbI_3$ perovskite orthorhombic-3D crystal lattice parameters, cell volume, density, effective coordination number (ECN), quadratic elongation (QE), bond angle variance (BAV), total energy per formula unit (E_{tot}), relative stabilization energy (R.E) wrt stable structure, and bandgap (E_g) calculated at PBE+D3 and $40\,\text{Å}^{-1}$.

Property	MA1	MA2	MA3
a_0 (Å)	8.91	9.27	9.38
b_0 (Å)	8.55	8.70	8.58
c_0 (Å)	12.73	12.57	12.52
α (°)	90.00	90.00	90.00
β (°)	90.00	90.00	90.00
γ (°)	90.00	90.00	90.00
V (Å^3/f.u)	242.25	253.47	252.08
Density (g cm^{-3})	4.25	4.06	4.08
Api. Oh rot. Pb–Pb–I (°)	10.14	0.05	10.57
Equi. Oh rot. Pb–Pb–I (°)	16.50	5.15	8.35
Equi1 Pb–I–Pb (°)	146.97	174.28	161.18
Equi2 Pb–I–Pb (°)	146.97	174.28	161.18
Api. Pb–I–Pb (°)	159.71	179.90	158.88
Oh torsion angle (°)	12.30	0.00	9.80
Pb(1) I_6 vol. (Å^3)	44.37	42.13	42.81
Pb(2) I_6 vol. (Å^3)	44.37	42.13	42.81
Pb(3) I_6 vol. (Å^3)	44.37	42.36	43.44
Pb(4) I_6 vol. (Å^3)	44.37	42.36	43.44
ECN^{Pb1}	6.00	5.96	5.98
ECN^{Pb2}	6.00	5.96	5.98
ECN^{Pb3}	6.00	5.92	5.97
ECN^{Pb4}	6.00	5.92	5.97
QE1	1.0043	1.0033	1.0200
QE2	1.0043	1.0033	1.0200
QE3	1.0043	1.0075	1.0081
QE4	1.0043	1.0075	1.0081
BAV1 (°^{2})	15.70	10.67	66.15
BAV2 (°^{2})	15.70	10.67	66.15
BAV3 (°^{2})	15.70	24.47	27.50
BAV4 (°^{2})	15.70	24.47	27.50
E_{tot} (eV)	−52.04	−51.86	−51.93
R.E (meV) per f.u	0	182	111
E_g (eV) at G (0,0,0)	1.76	1.50	1.76

5.5 $FAPbI_3$: Orthorhombic-3D Structure

Table 10: $FAPbI_3$ perovskite orthorhombic-3D crystal lattice parameters, cell volume, density, quadratic elongation (QE), effective coordination number (ECN), bond angle variance (BAV), total energy per formula unit (E_{tot}), relative stabilization energy (R.E) wrt stable structure, and bandgap (E_g) calculated at PBE+D3 and $40\,\text{Å}^{-1}$.

Property	FA1	FA2	FA3
a_0 (Å)	9.01	9.64	10.09
b_0 (Å)	8.90	8.46	8.02
c_0 (Å)	12.57	12.73	12.42
α (°)	90.00	90.00	90.02
β (°)	90.00	90.00	90.00
γ (°)	90.00	90.00	90.00
V (Å^3/f.u)	251.88	259.68	251.22
Density (g cm^{-3})	4.17	4.05	4.18
Api. Oh rot. Pb–Pb–I (°)	0.00	2.15	4.48
Equi. Oh rot. Pb–Pb–I (°)	14.93	4.61	9.79
Equi1 Pb–I–Pb (°)	150.13	166.71	149.95
Equi2 Pb–I–Pb (°)	150.13	170.85	160.22
Api. Pb–I–Pb (°)	180.00	175.70	4.48
Oh torsion angle (°)	0.00	0.00	0.00
Pb(1) I_6 vol. (Å^3)	42.06	43.28	41.87
Pb(2) I_6 vol. (Å^3)	42.06	43.28	41.87
Pb(3) I_6 vol. (Å^3)	44.90	43.28	41.87
Pb(4) I_6 vol. (Å^3)	44.90	43.28	41.87
ECN^{Pb1}	6.00	5.97	5.44
ECN^{Pb2}	6.00	5.97	5.44
ECN^{Pb3}	5.90	5.97	5.44
ECN^{Pb4}	5.90	5.97	5.44
QE1	1.0033	1.0132	1.0753
QE2	1.0033	1.0132	1.0753
QE3	1.0075	1.0132	1.0753
QE4	1.0075	1.0132	1.0753
BAV1 (°^{2})	0.18	45.15	225.57
BAV2 (°^{2})	0.18	45.15	225.57
BAV3 (°^{2})	0.17	45.15	225.57
BAV4 (°^{2})	0.17	45.15	225.57
E_{tot} (eV)	−56.77	−56.78	−54.63
R.E (meV) per f.u	6	0	2146
E_g (eV) at G (0,0,0)	1.49	1.67	0.91

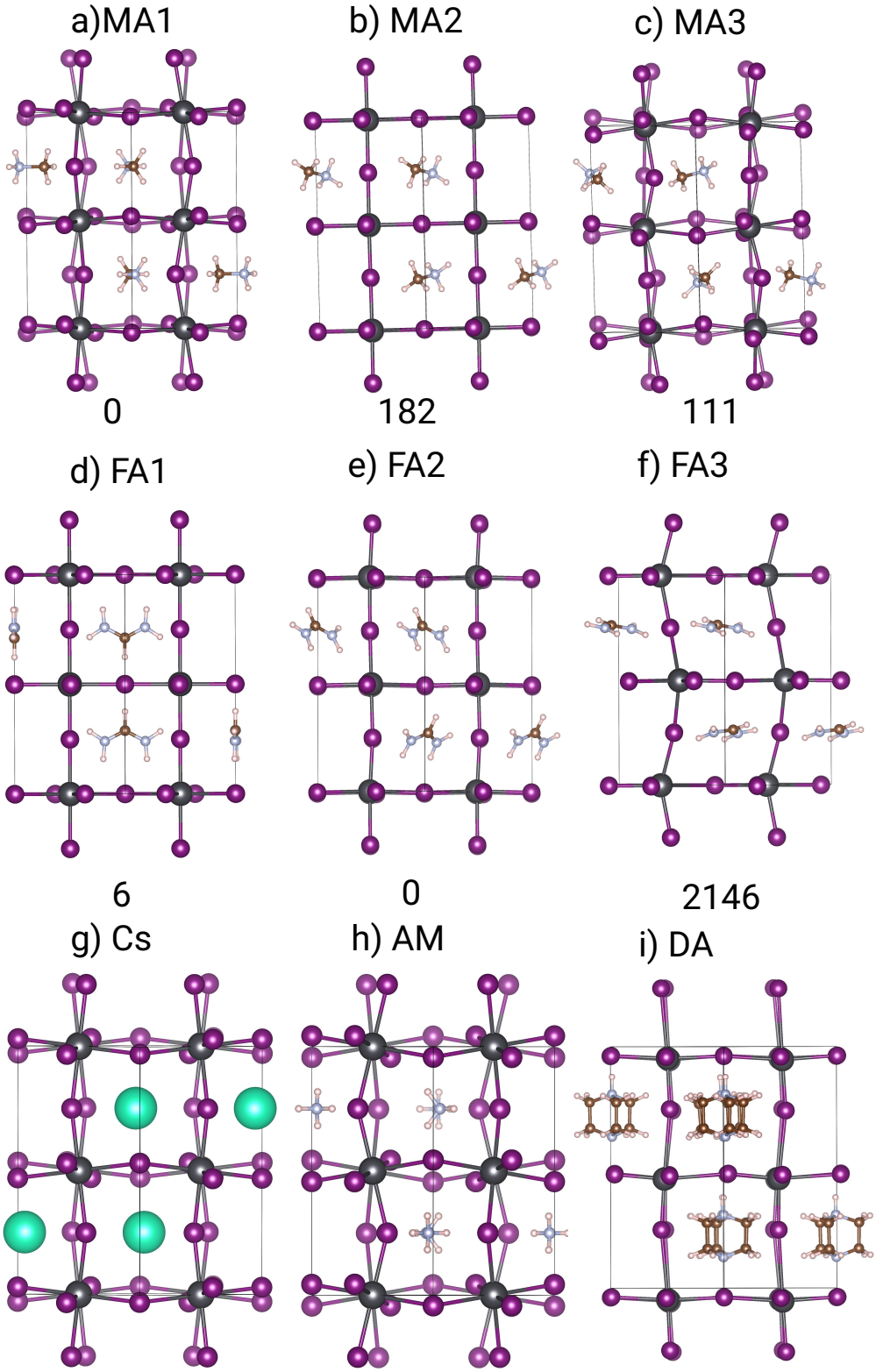

Figure 2: The orthorhombic (O3D) perovskites having the central inorganic and organic cation with distinct molecular orientations of a-c) methylammonium (MA), d-f) formamidinium (FA), g) Cs, h) ammonium (AM) and (i) dabconium (DA), respectively, relative stabilization energies are given in meV

5.6 $MAPbI_3$: Hexagonal Structure

Table 11: $MAPbI_3$ perovskite hexagonal crystal lattice parameters, cell volume, density, quadratic elongation (QE), effective coordination number (ECN), bond angle variance (BAV), total energy per formula unit (E_{tot}), relative stabilization energy (R.E) wrt stable structure, and bandgap (E_g) calculated at PBE+D3 and $40\,\text{Å}^{-1}$.

Property	MA1	MA2	MA3
a_0 (Å)	8.74	8.84	8.83
b_0 (Å)	8.49	8.47	8.48
c_0 (Å)	7.83	7.87	7.87
α (°)	92.71	96.09	82.58
β (°)	96.86	80.87	100.12
γ (°)	119.91	121.35	121.19
V (Å^3/f.u)	248.07	248.15	247.84
Density (g cm^{-3})	4.15	4.15	4.15
Pb(1) I_6 vol. (Å^3)	45.40	45.05	45.18
Pb(2) I_6 vol. (Å^3)	45.60	45.18	45.21
ECN^{Pb1}	5.99	5.94	5.95
ECN^{Pb2}	5.95	5.95	5.95
QE1	1.0035	1.0072	1.0079
QE2	1.0034	1.0072	1.0082
BAV1 ($^{\circ 2}$)	12.25	23.73	25.95
BAV2 ($^{\circ 2}$)	11.17	24.19	27.37
E_{tot} (eV)	−52.03	−52.01	−51.98
R.E (meV) per f.u	0	15	49
E_g (eV) at G (0,0,0)	2.99	2.95	2.94

5.7 $FAPbI_3$: Hexagonal Structure

Table 12: $FAPbI_3$ perovskite hexagonal crystal lattice parameters, cell volume, density, quadratic elongation (QE), effective coordination number (ECN), bond angle variance (BAV), total energy per formula unit (E_{tot}), relative stabilization energy (R.E) wrt stable structure, and bandgap (E_g) calculated at PBE+D3 and $40\,\text{Å}^{-1}$.

Property	FA1	FA2	FA3
a_0 (Å)	8.56 (8.66)	8.67	8.58
b_0 (Å)	8.68 (8.66)	8.59	8.81
c_0 (Å)	7.99 (7.90)	7.94	7.88
α (°)	86.27	87.33	94.14
β (°)	92.23	94.55	87.68
γ (°)	120.56	120.43	120.95
V (Å^3/f.u)	255.04	254.37	254.98
Density (g cm^{-3})	4.12	4.13	4.12
Pb(1) I_6 vol. (Å^3)	45.56	45.04	45.21
Pb(2) I_6 vol. (Å^3)	45.00	45.47	45.17
ECN^{Pb1}	5.82	5.94	5.87
ECN^{Pb2}	5.92	5.86	5.89
QE1	1.0035	1.0072	1.0079
QE2	1.0034	1.0072	1.0082
BAV1 (°^{2})	23.24	22.24	22.38
BAV2 (°^{2})	25.20	19.17	22.72
E_{tot} (eV)	−56.83	−56.83	−56.82
R.E (meV) per f.u	0	1	10
E_g (eV) at G (0,0,0)	2.99	2.96	2.82

5.8 $DAPbI_3$: Hexagonal Structure

Table 13: $DAPbI_3$ perovskite hexagonal crystal lattice parameters, cell volume, density, quadratic elongation (QE), effective coordination number (ECN), bond angle variance (BAV), total energy per formula unit (E_{tot}), relative stabilization energy (R.E) wrt stable structure, and bandgap (E_g) calculated at PBE+D3 and $40\,\text{Å}^{-1}$.

Property	DA1	DA2	DA3
a_0 (Å)	10.01	10.03	9.96
b_0 (Å)	10.01	10.02	9.97
c_0 (Å)	7.75	8.04	8.10
α (°)	90.00	90.04	90.69
β (°)	90.00	89.97	90.00
γ (°)	120.00	120.02	119.79
V (Å^3/f.u)	336.53	349.78	348.87
Density (g cm^{-3})	3.46	3.33	3.34
Pb(1) I_6 vol. (Å^3)	45.63	46.60	46.80
Pb(2) I_6 vol. (Å^3)	46.49	46.18	45.97
ECN^{Pb1}	6.00	6.00	5.96
ECN^{Pb2}	6.00	5.87	5.93
QE1	1.0035	1.0072	1.0079
QE2	1.0034	1.0072	1.0082
BAV1 ($^{\circ 2}$)	4.85	22.24	22.38
BAV2 ($^{\circ 2}$)	2.05	19.17	22.72
E_{tot} (eV)	−56.83	−56.83	−56.82
R.E (meV) per f.u	0	168	124
E_g (eV) at G (0,0,0)	2.99	2.96	2.82

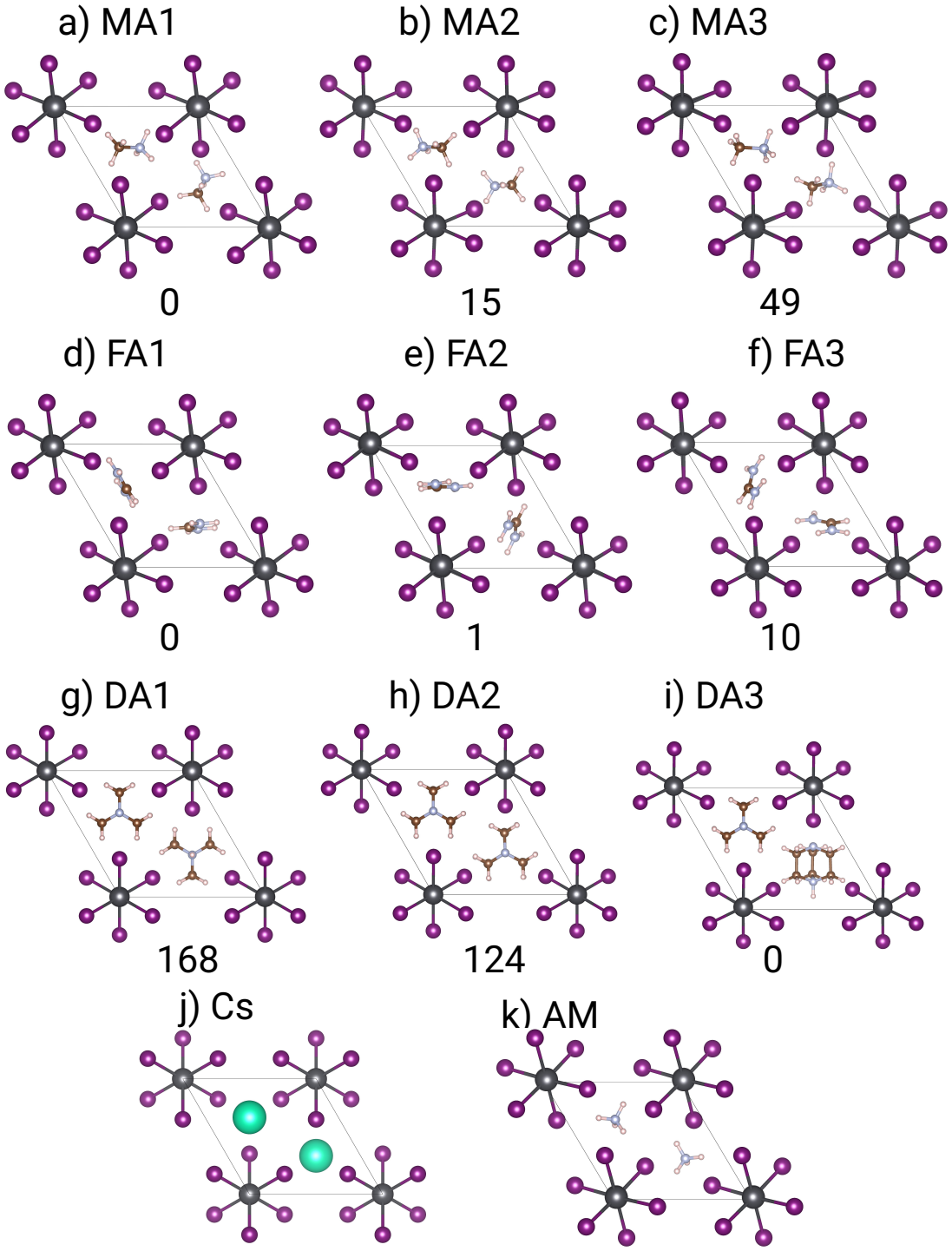

Figure 3: The hexagonal (2H) perovskites having the central cation of (a-c) methylammonium (MA), (d-f) formamidinium (FA), and (g-i) dabconium (DA), (j) Cs, (k) ammonium (AM) respectively, relative stabilization energies are given in meV**.**

5.9 $MAPbI_3$: Orthorhombic-1D Structure

Table 14: $MAPbI_3$ perovskite orthorhombic-1D crystal lattice parameters, cell volume, density, quadratic elongation (QE), effective coordination number (ECN), bond angle variance (BAV), total energy per formula unit (E_{tot}), relative stabilization energy (R.E) wrt stable, structure and bandgap (E_g) calculated at PBE+D3 and $40\,\text{Å}^{-1}$ kd

Property	MA1	MA2	MA3
a_0 (Å)	12.35	11.73	11.16
b_0 (Å)	4.72	4.74	4.70
c_0 (Å)	16.74	17.71	18.69
α (°)	90.00	90.00	90.00
β (°)	90.00	90.00	90.00
γ (°)	90.00	90.00	90.00
V (Å^3/f.u)	243.84	246.56	244.92
Density (g cm^{-3})	4.22	4.18	4.19
Pb(1) I_6 vol. (Å^3)	46.13	46.11	45.77
Pb(2) I_6 vol. (Å^3)	46.13	46.32	46.06
Pb(3) I_6 vol. (Å^3)	46.13	46.31	45.98
Pb(4) I_6 vol. (Å^3)	46.13	46.11	46.31
ECN^{Pb1}	5.67	5.77	5.75
ECN^{Pb2}	5.67	5.89	5.90
ECN^{Pb3}	5.67	5.89	5.82
ECN^{Pb4}	5.67	5.76	5.93
QE1	1.0083	1.0092	1.0068
QE2	1.0083	1.0082	1.0065
QE3	1.0083	1.0081	1.0072
QE4	1.0083	1.0092	1.0042
BAV1 (°^{2})	25.07	28.99	21.18
BAV2 (°^{2})	25.07	26.99	20.69
BAV3 (°^{2})	25.07	26.94	23.22
BAV4 (°^{2})	25.07	29.14	13.39
E_{tot} (eV)	−51.99	−51.99	−52.05
R.E (meV) per f.u	74	67	0
E_g (eV) at G (0,0,0)	2.70	2.77	2.84

5.10 $FAPbI_3$: Orthorhombic-1D Structure

Table 15: $FAPbI_3$ perovskite orthorhombic-1D crystal lattice parameters, cell volume, density, quadratic elongation (QE), effective coordination number (ECN), bond angle variance (BAV), total energy per formula unit (E_{tot}), relative stabilization energy (R.E) and bandgap (E_g) calculated at PBE+D3 and 40 $Å^{-1}$.

Property	FA1	FA2	FA3
a_0 (Å)	11.76	12.06	11.09
b_0 (Å)	4.55	4.56	4.59
c_0 (Å)	19.50	19.14	20.38
α (°)	90.00	90.00	90.00
β (°)	90.00	90.00	90.00
γ (°)	90.00	90.00	90.00
V (Å³/f.u)	260.53	263.10	259.47
Density ($g\,cm^{-3}$)	4.03	4.00	4.05
Pb(1) I_6 vol. (Å³)	46.22	47.16	46.35
Pb(2) I_6 vol. (Å³)	46.22	46.10	46.28
Pb(3) I_6 vol. (Å³)	46.22	47.19	46.26
Pb(4) I_6 vol. (Å³)	46.22	46.40	46.32
ECN^{Pb1}	5.81	5.28	5.76
ECN^{Pb2}	5.81	5.74	5.78
ECN^{Pb3}	5.81	5.28	5.79
ECN^{Pb4}	5.81	5.71	5.77
QE1	1.0024	1.0056	1.0060
QE2	1.0024	1.0036	1.0060
QE3	1.0024	1.0054	1.0057
QE4	1.0024	1.0049	1.0060
BAV1 (°²)	6.01	7.33	18.00
BAV2 (°²)	6.01	9.73	18.30
BAV3 (°²)	6.01	6.96	17.36
BAV4 (°²)	6.01	14.42	16.83
E_{tot} (eV)	−56.91	−56.82	−56.91
R.E (meV) per f.u	0	92	2
E_g (eV) at G (0,0,0)	3.15	3.07	3.11

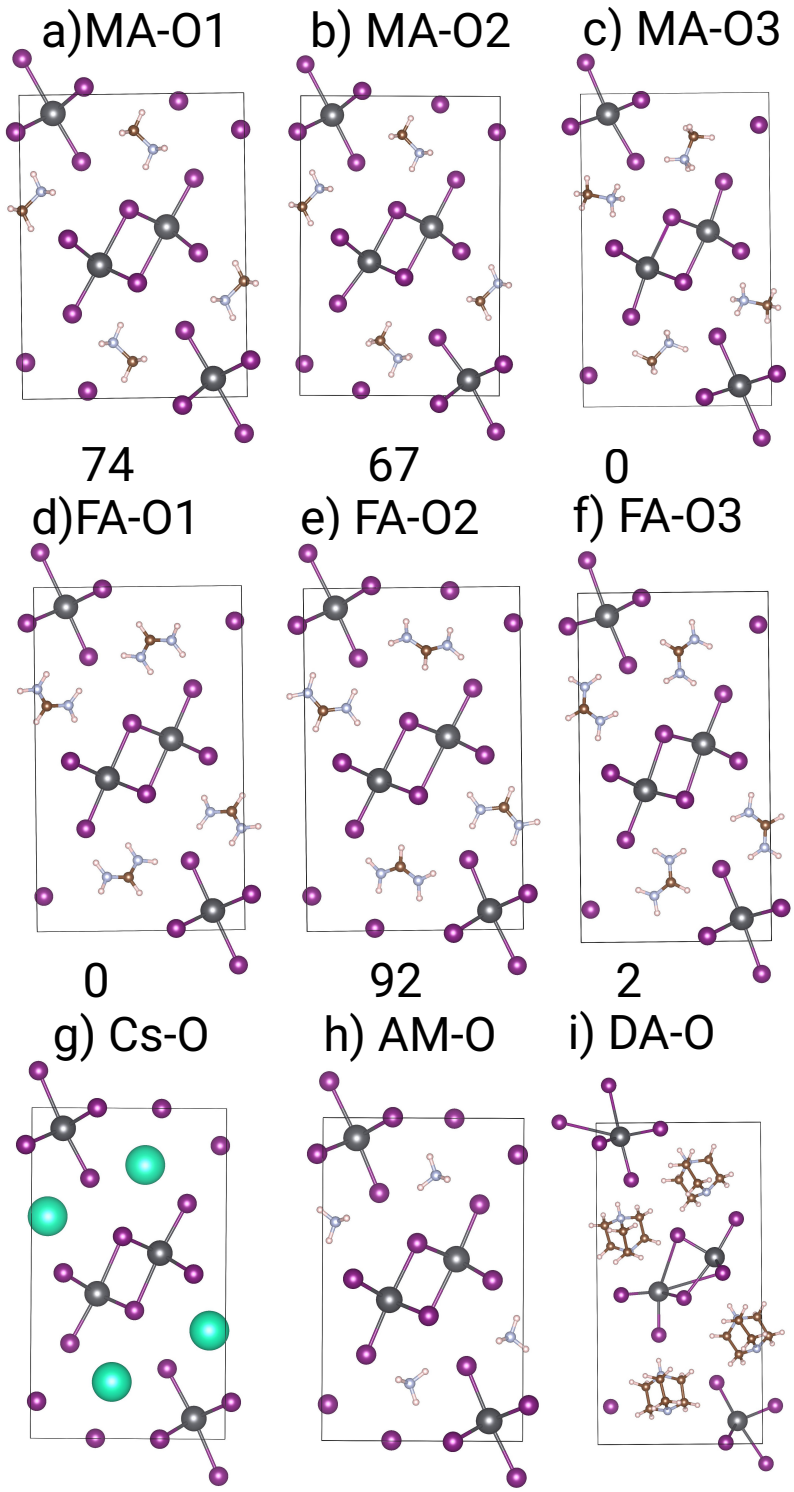

Figure 4: The orthorhombic (O1D) non-perovskite having the central inorganic and organic cation with distinct molecular orientations of a-c) methylammonium (MA), d-f) formamidinium (FA), g) Cs, h) ammonium (AM) and (i) dabconium (DA), respectively, relative stabilization energies are given in meV**.**

6 Structural Parameters, Energetic, and Electronic Properties for the Lowest Energy Configurations for the APbI$_3$ Structures for A = Cs, AM, MA, FA, DA

6.1 APbI$_3$: Cubic and Peseudo-cubic Structures

Table 16: APbI$_3$ perovskite cubic and pseudo-cubic crystal lattice parameters, cell volume, density, polyhedral ratio, discrepancy factor (d), quadratic elongation (QE), effective coordination number (ECN), bond angle variance (BAV), $\triangle x$-ionic displacement, cohesive energy, lattice energy, enthalpy of formation and bandgap, E_g, calculated at PBE+D3 and $40\,\text{Å}^{-1}$ (experimental measurements in parentheses).

	Property	Cs	AM	MA1	FA3	DA3
CUBIC/PSEUDO-CUBIC	a_0 (Å)	6.31 (6.29)	6.28	6.30 (6.31)	6.31 (6.36)	7.00
	b_0 (Å)	6.31 (6.29)	6.28	6.40 (6.31)	6.61 (6.36)	7.03
	c_0 (Å)	6.31 (6.29)	6.28	6.36 (6.31)	6.32 (6.36)	7.03
	Vol. (Å^3/f.u)	251.06 (249.64)	247.64	256.48 (251.60)	263.91	346.10
	Density (g cm^{-3})	4.77 (4.81)	4.06	4.01 (4.05)	3.98	3.36
	PbI$_6$ vol. (Å^3)	41.84 (41.61)	41.27	42.75	43.63	57.68
	AI$_{12}$ vol. (Å^3)	209.22 (208.03)	221.52	217.32	223.84	298.55
	Ratio (AI$_{12}$/PbI$_6$)	5.00	5.37	5.08	5.09	5.18
	d^{Pb}	0.498	0.256	0.288	0.219	−0.087
	ECN^{Pb}	6.00	6.00	5.89	5.57	3.09
	Avg. Pb–I (Å)	3.15	3.19	3.19	3.22	3.52
	Avg. Pb–I–Pb (°)	180.00	159.25	168.73	169.20	160.69
	QE	1.0000	1.0335	1.0104	1.0119	1.0284
	BAV (°^{2})	0.00	115.03	35.49	33.18	28.39
	$\triangle A$ (in Å)	0.00	0.55	0.52	0.25	0.36
	$\triangle Pb$ (in Å)	0.00	0.30	0.15	0.25	0.44
	$\triangle I$ (in Å)	0.00	0.64	0.43	0.17	0.47
	E_{coh} per atom (eV)	−2.81	−2.94	−3.30	−4.06	−4.02
	$\triangle H$ (kJ/mol)	−237.34	42.13	11.59	24.17	6.07
	E_g (eV) at R (0.5,0.5,0.5)	1.36	2.02	1.63	1.64	2.13
	E_g (eV) at G (0,0,0)	4.28	3.68	4.50	3.80	4.41

6.2 APbI$_3$: Hexagonal and Pseudo-hexagonal Structures

Table 17: APbI$_3$ perovskite hexagonal/pseudo-hexagonal crystal lattice parameters, cell volume per f.u, density, and enthalpy of formation calculated, total energy per formula unit, E_{tot}, relative stabilization energy (R.E) wrt cubic structure and bandgap, E_g, calculated at PBE+D3 and $40\,\text{Å}^{-1}$. The experimental measurements are in parentheses.

	Property	Cs	AM	MA1	FA1	DA1
HEXAGONAL/PSEUDO-HEXAGONAL	a_0 (Å)	8.60	8.37	8.74	8.56	10.01
					(8.59)	(10.48)
	b_0 (Å)	8.60	8.36	8.49	8.68	10.01
					(8.59)	(10.48)
	c_0 (Å)	7.57	7.88	7.83	7.99	7.75
					(7.85)	(8.11)
	α (°)	90.00	95.00	92.71	86.27	90.00
	β (°)	90.00	92.49	96.86	92.23	90.00
	γ (°)	120.00	120.33	119.31	120.56	120.00
	Vol. (Å^3/f.u)	242.35	235.74	248.07	255.04	336.53
	Density ($\text{g}\,\text{cm}^{-3}$)	4.91	4.27	4.15	4.12	3.46
					(4.19)	
	Pb(1) I_6	44.78	45.52	45.40	45.56	45.63
	Pb(2) I_6	44.78	45.66	45.60	45.00	46.49
	ECN^{Pb1}	6.00	5.98	5.99	5.82	6.00
	ECN^{Pb2}	6.00	5.98	5.95	5.92	6.00
	QE1	1.0003	1.0032	1.0035	1.0071	1.0013
	QE2	1.0003	1.0031	1.0034	1.0072	1.0006
	BAV1 ($^{\circ 2}$)	0.94	11.20	12.25	23.24	4.85
	BAV2 ($^{\circ 2}$)	0.94	10.97	11.17	25.20	2.05
	E_{coh} per atom (eV)	−2.82	−2.99	−3.31	−4.08	−4.03
	$\triangle H$ (kJ/mol)	−244.50	3.77	−2.21	3.11	−12.96
	R.E ($\text{kJ}\,\text{mol}^{-1}$) per f.u	−7.16	−38.36	−13.79	−21.06	−19.03
	E_g (eV) at G (0,0,0)	2.53	3.42	2.99	2.99	2.56

6.3 APbI$_3$: Non-perovskite orthorhombic-1D Structure

Table 18: APbI$_3$ non-perovskite orthorhombic-1D crystal lattice parameters, cell volume per f.u, density, and enthalpy of formation, total energy per formula unit, E_{tot}, and relative stabilization energy (R.E) wrt cubic structure calculated at PBE+D3 and $40\,\text{Å}^{-1}$. The experimental measurements are in parentheses.

	Property	Cs	AM	MA3	FA1	DA
ORTHORHOMBIC-1D	a_0 (Å)	10.64 (10.43)	10.57 (10.30)	11.16	11.76	11.31
	b_0 (Å)	4.84 (4.79)	4.76 (4.74)	4.70	4.55 6.13	
	c_0 (Å)	18.08 (17.76)	17.02 (17.29)	18.69	19.50	22.09
	α (°)	90.00	90.00	90.00	90.00	90.00
	β (°)	90.00	90.00	90.00	90.00	90.00
	γ (°)	90.00	90.00	90.00	90.00	90.00
	V (Å^3/f.u)	232.76	214.16	244.92	260.53	383.09
	Density ($\text{g}\,\text{cm}^{-3}$)	5.14 (5.39)	4.70 (4.22)	4.20	4.03	3.04
	Pb(1) I_6	46.18	45.24	45.80	46.22	46.93
	ECN^{Pb1}	5.75	5.93	5.75	5.81	3.35
	ECN^{Pb2}	5.75	5.93	5.90	5.81	3.41
	ECN^{Pb3}	5.75	5.93	5.82	5.81	4.09
	ECN^{Pb4}	5.75	5.93	5.93	5.81	3.00
	QE1	1.0062	1.0045	1.0068	1.0024	1.3761
	BAV1 (°^{2})	12.64	13.90	21.18	6.01	
	E_{coh} per atom (eV)	−2.83	−3.00	−3.31	−4.08	−4.00
	$\triangle H$ (kJ/mol)	−249.19	−9.48	−4.26	−4.10	−12.54
	R.E ($\text{kJ}\,\text{mol}^{-1}$) per f.u	−11.86	−51.61	−16.81	−28.27	41.75
	E_g (eV) at G (0,0,0)	2.76	2.81	2.77	3.15	2.98

6.4 APbI$_3$: Orthorhombic-3D Structure

Table 19: APbI$_3$ perovskite orthorhombic-3D crystal lattice parameters, cell volume per f.u, density, and enthalpy of formation calculated, total energy per formula unit, E_{tot}, relative stabilization energy (R.E) wrt cubic structure at PBE+D3 and 40 Å^{-1} (experimental measurements in parentheses).

	Property	Cs	AM	MA1	FA2	DA
ORTHORHOMBIC-3D	a_0 (Å)	8.82	8.58	8.91	8.46	9.63
		(8.62)		(8.84)		
	b_0 (Å)	8.76	8.61	8.55	9.64	9.74
		(8.85)		(8.56)		
	c_0 (Å)	12.66	12.47	12.73	12.73	15.13
		(12.50)		(12.59)		
	α (°)	90.00	90.00	90.00	90.00	90.00
	β (°)	90.00	90.00	90.00	90.00	90.00
	γ (°)	90.00	90.00	90.00	90.00	90.00
	V (Å^3/f.u)	244.66	230.16	242.25	259.68	354.71
	Density (g cm^{-3})	4.89	4.37	4.25	4.05	3.28
		(5.02)		(4.32)		
	Api. Oh rot. Pb–Pb–I (°)	8.97	14.31	10.14	2.15	5.63
	Equi. Oh rot. Pb–Pb–I (°)	13.05	18.97	16.53	4.61	10.29
	Equi1 Pb–I–Pb (°)	153.85	142.05	146.97	170.84	161.89
	Equi2 Pb–I–Pb (°)	153.85	142.05	146.97	166.70	164.75
	Api. Pb–I–Pb (°)	162.06	151.37	159.71	175.70	165.79
	Oh torsion angle (°)	11.42	15.91	12.30	0.00	121.28
	Pb(1) I$_6$	43.47	44.23	44.37	43.28	57.59
	ECN^{Pb1}	6.00	6.00	6.00	5.97	3.19
	QE1	1.0006	1.0006	1.0043	1.0132	1.0525
	BAV1 (°^{2})	1.99	2.17	15.70	45.15	82.95
	E_{coh} per atom (eV)	−2.82	−2.99	−3.31	−4.07	−4.01
	$\triangle H$ (kJ/mol)	−241.50	−0.02	−3.63	8.42	28.02
	R.E (kJ mol^{-1}) per f.u	−4.16	−44.02	−15.22	−15.75	26.23
	E_g (eV) at G	1.63	1.87	1.76	1.67	2.07

7 APbI$_3$: Octahedral Volume Changes

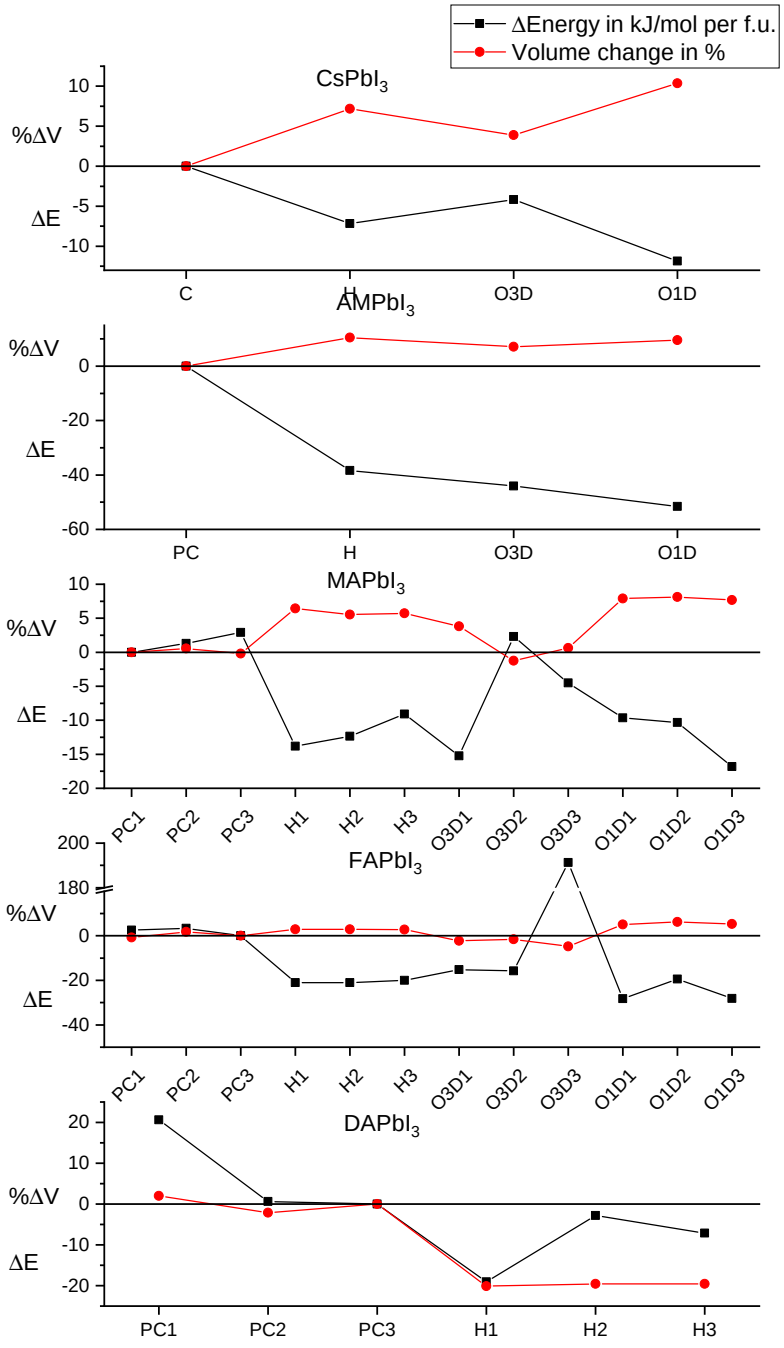

Figure 5: Percentage of change in octahedral volumes among different polytypes of APbI$_3$, PbI$_6$ volume of cubic/pseudo-cubic structure taken as reference

8 Perovskites Optical Properties

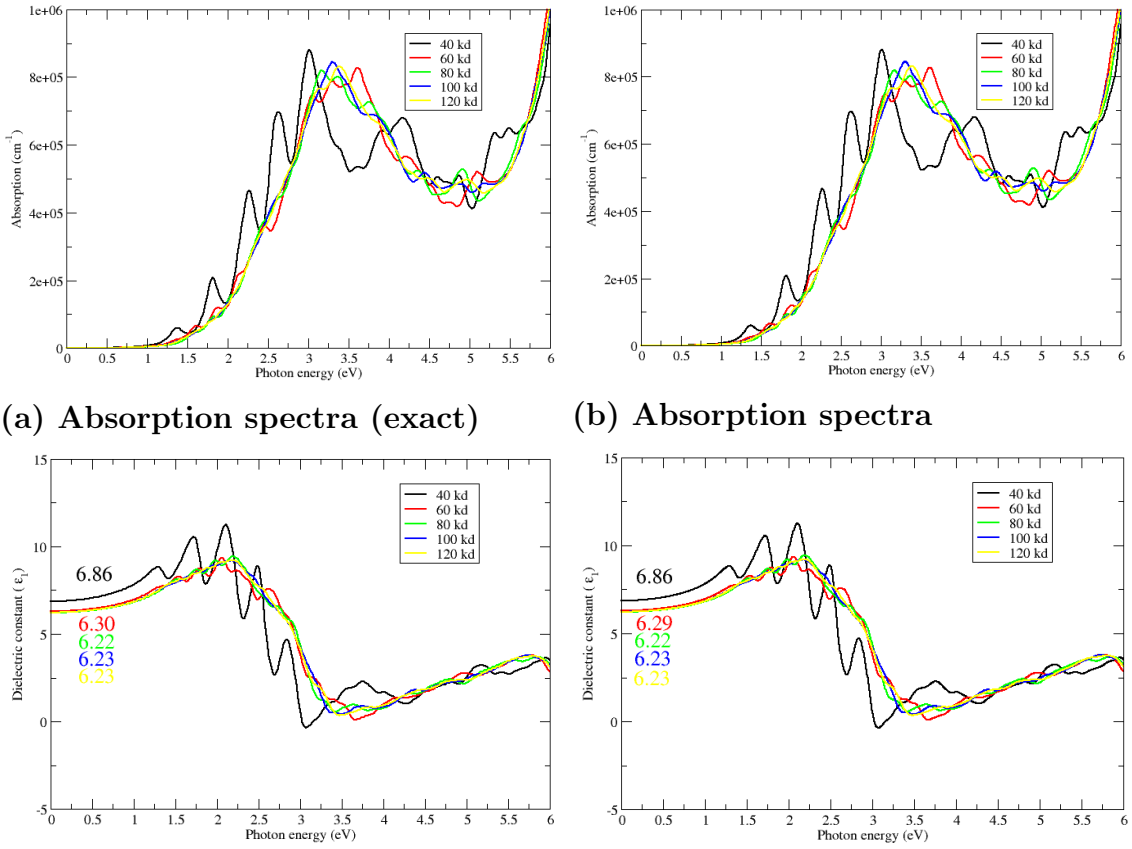

(a) Absorption spectra (exact) (b) Absorption spectra

(c) Real dielectric constant (exact) (d) Real dielectric constant

Figure 6: Computational study of the convergence of the dielectric functions as a function of the number of k-points for the cubic $CsPbI_3$ structure: (a) absorption spectra using a `CSHIFT` of $0.1\,\mathrm{eV}$ (`ALGO` = `Exact`, `NELM` = 1), (b) Absorption spectra using a `CSHIFT` of $0.1\,\mathrm{eV}$ (`ALGO` = `Normal`), c) real dielectric constant (`ALGO` = `Exact`, `NELM` = 1), d) real dielectric constant (`ALGO` = `Normal`).

Table 20: Energy gap (in eV), transition type and transition amplitude (a.u.) at high symmetrical k-points of cubic/PC $APbI_3$ compounds

C/PC	Band	Energy	Type	Amplitude	k-point
Cs	23-24	1.36	(1,1)	20.78	(0.50,0.50,0.50)
	23-24	1.36	(2,2)	20.81	(0.50,0.50,0.50)
	23-24	1.36	(3,3)	3.94	(0.50,0.50,0.50)
	23-24	1.36	(1,3)	-9.05	(0.50,0.50,0.50)
	23-24	1.40	(2,2)	43.92	(0.47,0.50,0.47)
AM	23-24	2.02	(1,1)	5.64	(0.50,0.50,0.50)
	23-24	2.02	(2,2)	5.97	(0.50,0.50,0.50)
	23-24	2.02	(3,3)	5.94	(0.50,0.50,0.50)
MA1	26-27	1.63	(1,1)	0.00	(0.50,0.50,0.50)
	26-27	1.63	(2,2)	14.21	(0.50,0.50,0.50)
	26-27	1.63	(3,3)	7.67	(0.50,0.50,0.50)
FA1	28-29	1.42	(1,1)	0.00	(0.50,0.50,0.50)
	28-29	1.42	(2,2)	0.00	(0.50,0.50,0.50)
	28-29	1.42	(3,3)	20.91	(0.50,0.50,0.50)
FA3	28-29	1.64	(1,1)	7.74	(0.47,0.47,0.47)
	28-29	1.64	(1,1)	7.59	(0.50,0.50,0.50)
DA3	42-43	2.18	(1,1)	0.02	(0.50,0.50,0.50)
	42-43	2.18	(2,2)	0.02	(0.50,0.50,0.50)
	42-43	2.18	(2,2)	0.01	(0.50,0.50,0.50)
	42-43	2.31	(3,3)	0.19	(0.50,0.50,0.00)

Table 21: Energy gap (in eV), transition type and transition amplitude (a.u.) at high symmetrical k-points of orthorhombic-3D $APbI_3$ compounds

O3D	Band	Energy	Type	Amplitude	k-point
Cs	92-93	1.63	(1,1)	0.00	(0.00,0.00,0.00)
	92-93	1.63	(2,2)	0.00	(0.00,0.00,0.00)
	92-93	1.63	(3,3)	6.88	(0.00,0.00,0.00)
AM	92-93	1.87	(1,1)	0.00	(0.00,0.00,0.00)
	92-93	1.87	(2,2)	4.08	(0.00,0.00,0.00)
	92-93	1.87	(3,3)	0.00	(0.00,0.00,0.00)
MA1	104-105	1.76	(1,1)	0.00	(0.00,0.00,0.00)
	104-105	1.76	(2,2)	5.12	(0.00,0.00,0.00)
	104-105	1.76	(3,3)	0.00	(0.00,0.00,0.00)
FA2	112-113	1.67	(1,1)	0.00	(0.00,0.00,0.00)
	112-113	1.67	(2,2)	7.96	(0.00,0.00,0.00)
	112-112	1.67	(3,3)	0.01	(0.00,0.00,0.00)
DA	168-169	2.18	(1,1)	0.00	(0.00,0.00,0.00)
	168-169	2.18	(2,2)	0.00	(0.00,0.00,0.00)
	168-169	2.18	(3,3)	0.00	(0.00,0.00,0.00)
	168-169	2.38	(2,2)	0.01	(0.50,0.50,0.00)

Table 22: Energy gap (in eV), transition type and transition amplitude (a.u.) at high symmetrical k-points of orthorhombic-1D $APbI_3$ compounds

O1D	Band	Energy	Type	Amplitude	k-point
Cs	92-93	2.56	(1,1)	0.00	(0.39,0.00,0.00)
	92-93	2.56	(2,2)	0.00	(0.39,0.00,0.00)
	92-93	2.56	(3,3)	0.21	(0.39,0.00,0.00)
AM	92-93	2.43	(1,1)	0.00	(0.42,0.00 0.00)
	92-93	2.43	(2,2)	0.00	(0.0,0.00,0.00)
	92-93	2.43	(3,3)	0.29	(0.00,0.00,0.00)
MA1	104-105	2.45	(1,1)	0.00	(0.50,0.00,0.00)
	104-105	2.45	(2,2)	0.00	(0.50,0.00,0.00)
	104-105	2.45	(3,3)	0.00	(0.50,0.00,0.00)
	104-105	2.46	(1,1)	0.03	(0.50,0.00,0.50)
FA2	112-113	2.89	(1,1)	0.00	(0.42,0.00,0.00)
	112-113	2.89	(2,2)	0.01	(0.42,0.00,0.00)
	112-112	2.89	(3,3)	0.22	(0.42,0.00,0.00)
DA	168-169	2.67	(1,1)	0.01	(0.00,0.34,0.00)
	168-169	2.67	(2,2)	0.01	(0.00,0.34,0.00)
	168-169	2.67	(3,3)	0.00	(0.00,0.34,0.00)

Table 23: Energy gap (in eV), transition type and transition amplitude (a.u.) at high symmetrical k-points of hexagonal $APbI_3$ compounds

H	Band	Energy	Type	Amplitude	k-point
Cs	46-47	2.53	(1,1)	0.00	(0.00,0.00,0.00)
	46-47	2.53	(2,2)	0.00	(0.00,0.00,0.00)
	46-47	2.53	(3,3)	0.00	(0.00,0.00,0.00)
	46-47	2.60	(1,1)	0.92	(0.50,0.00,0.00)
AM	46-47	3.07	(1,1)	0.25	(0.50,0.00,0.00)
	46-47	3.07	(2,2)	0.04	(0.50,0.00,0.00)
	46-47	3.07	(3,3)	0.01	(0.50,0.00,0.00)
MA1	52-53	2.99	(1,1)	0.21	(0.00,0.00,0.00)
	52-53	2.99	(2,2)	1.14	(0.00,0.00,0.00)
	52-53	2.99	(3,3)	0.02	(0.00,0.00,0.00)
FA1	56-57	2.99	(1,1)	0.11	(0.00,0.00,0.00)
	56-57	2.99	(2,2)	0.00	(0.00,0.00,0.00)
	56-57	2.99	(3,3)	0.00	(0.00,0.00,0.00)
DA1	84-85	2.55	(1,1)	0.00	(0.00,0.00,0.05)
	84-85	2.55	(2,2)	0.00	(0.00,0.00,0.05)
	84-85	2.55	(3,3)	0.00	(0.00,0.00,0.05)
	84-85	2.56	(3,3)	0.01	(0.00,0.00,0.13)

Table 24: Formation enthalpies (in eV) of $CsPbI_3$ polymorphs and pseudo-cubic $MAPbI_3$ unit-cell. (Note: Enthalpies of PBE+SOC functional calculated by doing single point energies on PBE optimized geometries of CsI, PbI_2 and $CsPbI_3$)

$CsPbI_3$	PBE	PBE+SOC	PBE+D3
Cubic	0.01	−0.02	−0.10
O3D	−0.11	−0.13	−0.15
O1D	−0.16	−0.17	−0.23
H	−0.07	−0.08	−0.18
$MAPbI_3$	PBE	PBE+SOC	PBE+D3
PC	0.04	0.01	0.12

References

(1) Goldschmidt, V. M. Die Gesetze der Krystallochemie. *Die Naturwissenschaften* **1926**, *14*, 477–485.

(2) Kieslich, G.; Sun, S.; Cheetham, A. K. An extended Tolerance Factor approach for organic–inorganic perovskites. *Chemical Science* **2015**, *6*, 3430–3433.

(3) Hoppe, R. Effective coordination numbers (ECoN) and mean fictive ionic radii (MEFIR). *Zeitschrift für Kristallographie - Crystalline Materials* **1979**, *150*, 23.

(4) Hoppe, R. The Coordination Number– an"Inorganic Chameleon". *Angewandte Chemie International Edition in English* **1970**, *9*, 25–34.

(5) McLeod, J. A.; Wu, Z.; Sun, B.; Liu, L. The influence of the I/Cl ratio on the performance of CH3NH3PbI3-xClx-based solar cells: why is CH3NH3I : PbCl2 = 3 : 1 the "magic" ratio? *Nanoscale* **2016**, *8*, 6361–6368.

(6) Robinson, K.; Gibbs, G. V.; Ribbe, P. H. Quadratic Elongation: A Quantitative Measure of Distortion in Coordination Polyhedra. *Science* **1971**, *172*, 567–570.

(7) Gajdoš, M.; Hummer, K.; Kresse, G.; Furthmüller, J.; Bechstedt, F. Linear optical properties in the projector-augmented wave methodology. *Physical Review B* **2006**, *73*, 045112.

(8) Ehrenreich, H.; Cohen, M. H. Self-Consistent Field Approach to the Many-Electron Problem. *Physical Review* **1959**, *115*, 786–790.

(9) Baroni, S.; de Gironcoli, S.; Corso, A. D.; Giannozzi, P. Phonons and related crystal properties from density-functional perturbation theory. *Reviews of Modern Physics* **2001**, *73*, 515–562.

(10) Sabino, F. P.; Besse, R.; Oliveira, L. N.; Wei, S.-H.; Silva, J. L. F. D. Origin of and tuning the optical and fundamental band gaps in transparent conducting oxides: The case ofM2O3(M=Al, Ga, In). *Physical Review B* **2015**, *92*, 205308.